



# Journal of Applied Sciences

ISSN 1812-5654

**science**  
alert

**ANSI***net*  
an open access publisher  
<http://ansinet.com>

## Comprehensive Analysis of a High-Q, Low Motional Resistance, Very High Frequency MEMS Resonator

<sup>1</sup>F. Babazadeh and <sup>2</sup>S.H. Keshmiri

<sup>1</sup>Department of Electrical Engineering,

<sup>2</sup>Departments of Electrical Engineering and Physics, Faculty of Engineering, Ferdowsi University, Mashhad, 91775-1111, Iran

**Abstract:** In this study, design and simulation of an IC-compatible microelectromechanical resonator for use in VHF range of a wireless communication system as a base element in integrated micromechanical resonator based oscillators and front-end filters is reported. This resonator can be implemented using thick polysilicon technology. The resonator with new design and structure reduces vibrating micromechanical series motional resistance  $R_x$  by increasing electrode-to-resonator overlap area through use of scale up of the motionless dimension of the device; while maintaining the resonant frequency. Quarter-wavelength supporting and attaching to nodal points of the resonator is required to maximize quality factor of the device. Resonant frequencies around 71 MHz, quality factor of 9912 and motional resistances  $R_x$  on the order of 480  $\Omega$  were obtained by this design.

**Key words:** Microelectromechanical systems, mechanical resonator, motional impedance, quality factor

### INTRODUCTION

Miniaturization of the constituent components of super-heterodyne wireless transceivers is a field of research that has received considerable attention recently. To date, several of these components can already be miniaturized using integrated circuit transistor technologies. Reduced size constitutes the most obvious incentive for replacing SAWs and crystals by equivalent devices. Typically, the front-end of a wireless transceiver contains a good number of off-chip high-Q components that are potentially replaceable by micromechanical versions. Among the components targeted for replacement are RF filters, including image reject filters (with center frequencies ranging from 800 MHz to 2.5 GHz), IF filters (with center frequencies ranging from 455 kHz to 254 MHz) and high-Q low phase-noise local oscillators with frequency requirements in the 10 MHz to 2.5 GHz range (Nguyen, 1998, 1999; De Los Santos, 2002). One of the challenging issues which has hindered deployment of the microelectromechanical resonators and filters is large motional resistance  $R_x$  of these devices with electrostatically and capacitively transduction.

Among methods for lowering the motional resistance  $R_x$  of electrostatically and capacitively

transduced micromechanical resonators presented so far are: (1) decreasing the electrode-to-resonator gap (Bannon III *et al.*, 2000), (2) increasing the dc-bias voltage  $V_p$  and (3) summing together the output currents of an array of identical resonators (Demirci *et al.*, 2003). Unfortunately, each of these methods comes with some drawbacks. In particular, although the first two methods are very effective in lowering  $R_x$  (with fourth power and square law dependencies, respectively), they do so at the cost of linearity (Navid *et al.*, 2001; Alastalo and Kaajakari, 2006). On the other hand, method (3) actually improves linearity while lowering  $R_x$ . However, this method is difficult to implement; since it requires resonators with precisely identical responses and consumes large area of silicon chip; since it uses an array of resonators instead of a single resonator.

This study presents a novel method for lowering motional resistance based on a technique which utilizes true potential of a single square frame resonator in three-dimensions and raises the linearity as well. Using this new technique, a simply-supported square frame microelectromechanical resonator (with an effective  $R_x$  of 478 k $\Omega$ ) was designed and simulated at 71 MHz. This effective resistance is about 75X smaller than the 35.9 k $\Omega$  exhibited by a 72 MHz Clamped-Clamped beam resonator (Varadan and Vinoy, 2002), 73X smaller than the 34.8 k $\Omega$

demonstrated by a 71 MHz free-free beam resonator (Wang *et al.*, 2000) and 8.4X smaller than the 4kΩ presented by a 68.1 MHz mechanically-coupled 11-resonators array (Demirci *et al.*, 2003).

This  $R_x$ -reduction method is superior to methods based on scaling down of electrode-to-resonator gaps, dc-bias increases, or using an array of identical resonators; because it allows a reduction in  $R_x$  without sacrificing linearity and consuming large chip area.

### MATERIALS AND METHODS

**Resonator structure and operation:** Figure 1 shows schematic top view of the proposed micromechanical resonator (along with appropriate bias, excitation and sensing circuitry). This resonator consists of a simply-supported square frame resonators, supported by four tethers and attached to substrate only at anchors, all suspended above the substrate.

To operate this resonator, a dc-bias  $V_p$  is applied to the suspended resonator structure and two complement ac input voltages  $v_i$  and  $-v_i$  are applied to the input electrodes, which are placed by a 100 nm gap from the structures, as shown in Fig. 1. The application of input voltages  $v_i$  and  $-v_i$  creates x- and y-directed electrostatic forces between input electrodes and the conductive resonator that induce x- and y-directed vibration of the input resonator when the frequency of the input voltage comes equal to the resonant frequency of the mechanical resonator. Vibration of the square frame resonator creates a dc-biased, time-varying capacitor between the conductive resonator and electrodes, which then sources an output current given by:

$$i_o = V_p \left( \frac{\partial C}{\partial x} \right) \left( \frac{\partial x}{\partial t} \right) \quad (1)$$

where,  $\partial C/\partial x$  is the change in resonator-to-electrode capacitance per unit displacement at input ports. The output current  $i_o$  is then directed to resistor  $R_i$ , which converts the current to output voltage.

Since, center frequency of a given mechanical filter and oscillation frequency of a given oscillator are determined primarily by the resonance frequencies of its constituent resonators, careful mechanical resonator design is imperative for successful device implementation. The selected resonator design must not only be able to achieve the needed frequency but must also do so with adequate linearity and tunability and with sufficient Q.

As shown in Fig. 2, the microresonator is formed of four polysilicon beams which are attached to each other and organized in a square frame. Other polysilicon tethers

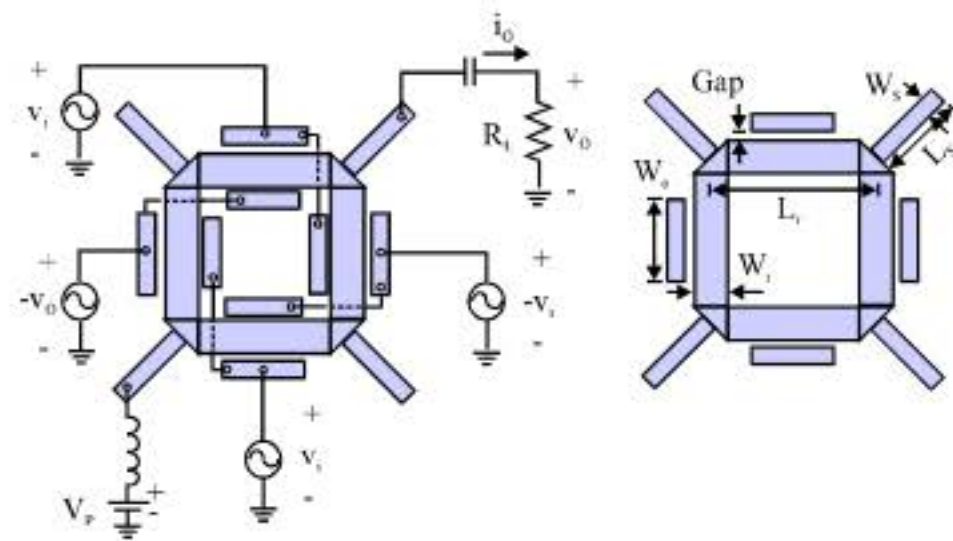


Fig. 1: Top view schematic of a square frame micromechanical resonator, along with the preferred bias, excitation and sensing circuitry

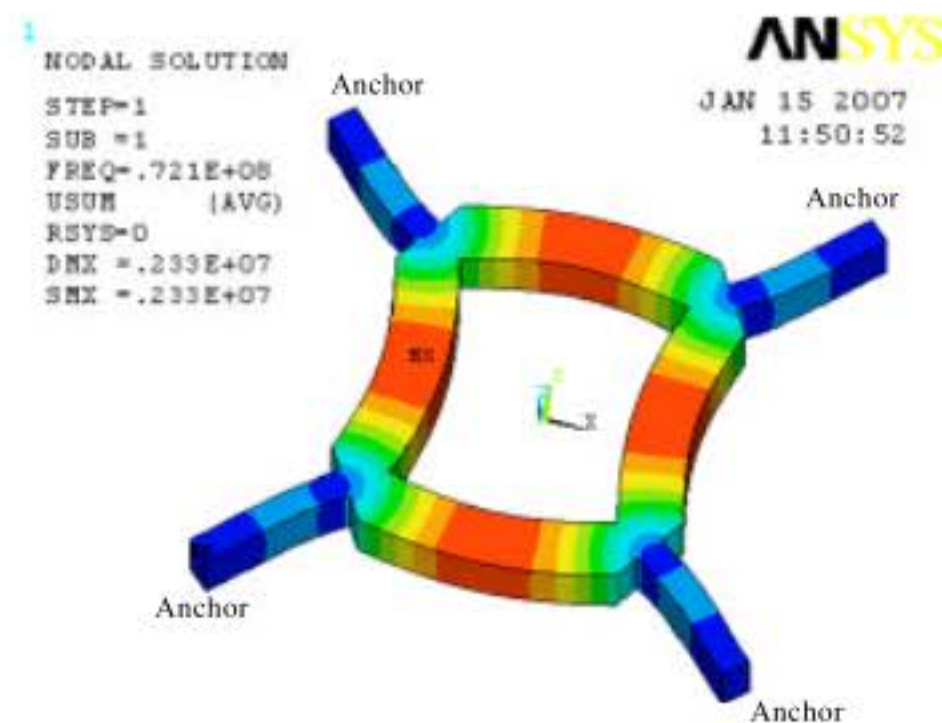


Fig. 2: Fundamental mode shape of the micromechanical resonator simulated by ANSYS

attach corners of this frame to anchors. The anchors are tightly placed on substrate and cause the whole structure to suspend above the substrate with a little space between them. This polysilicon square frame can freely move parallel to substrate in x and y orientations.

The resonance frequency of this simply-supported square frame depends upon many factors, including geometry, structural material properties, stress, the magnitude of the applied dc-bias voltage  $V_p$  and surface topography.

Accounting for these while neglecting finite width effects, an expression for resonance frequency can be written as (Timoshenko *et al.*, 1974):

$$f_{\text{nom}} = \frac{\beta_n^2}{4\pi\sqrt{3}} \kappa \frac{W_r}{L_r^2} \sqrt{\frac{E}{\rho}} \quad (2)$$

where  $W_r$  and  $L_r$  are the width and effective length of the beam, respectively, E is the Young's modulus,  $\rho$  is the

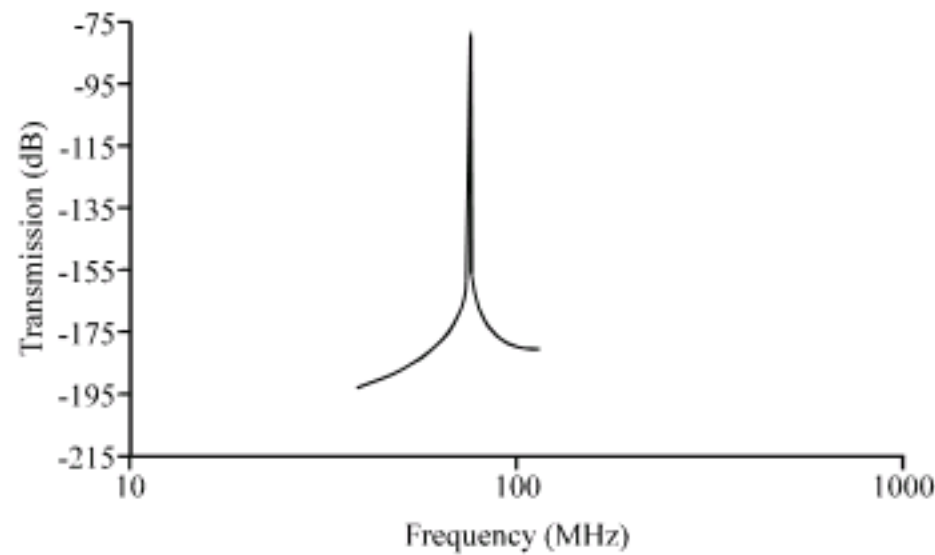


Fig. 3: Mechanical frequency response of the microresonator

density of the structural material,  $\beta_n = 3.1415, 6.2831, 9.4247$  for the first three modes of a simply-supported beam,  $f_{nom}$  is the nominal mechanical resonance frequency of the resonator if there were no electrodes or applied voltages and  $\kappa$  is a scaling factor that models the effects of surface topography.

Mechanical frequency response of the designed resonator is shown in Fig. 3.

To properly excite this device, a voltage consisting of a dc-bias  $V_p$  and an ac excitation  $v_i$  is applied across one of the resonator-to-electrode capacitors (i.e., the input transducer). This creates a force component between the electrode and resonator proportional to the product  $V_p v_i$  and at the frequency of  $v_i$ . When the frequency of  $v_i$  nears its resonance frequency, the microresonator begins to vibrate, creating a dc-biased time-varying capacitor  $C_0(x,t)$  at the input transducer. A current is then generated through the output transducer and serves as the output of this device. When plotted against the frequency of the excitation signal  $v_i$ , the output current  $i_o$  traces out the bandpass biquad characteristic expected for a high-Q tank circuit.

It must be noted that from the discussion associated with Eq. 1, the effective input force ( $\sim V_p v_i$ ) and output current can be nulled by setting  $V_p = 0$ . Thus, a micromechanical resonator (and oscillator or filter constructed of such resonators) can be switched in and out by the mere application and removal of the dc-bias voltage  $V_p$ . Such switchability can be used to great advantage in receiver architectures.

Design of the micromechanical resonator in form of Fig. 2, has some advantages as follows:

- The fully-differential electrode configuration cancels the second harmonic distortion term ( $HD_2$ ); therefore, improves the power-handling capability and dynamic range of the resonator

- The present structure design, decreases input and output impedances significantly and in filter design case, matches the impedance of filter to the impedances of the stages before and after the filter, properly
- Since, the proposed resonator structure has four almost motionless node points, the quality factor due to energy loss mechanisms of support loss ( $Q_{Support}$ ) is high and hence Q of the whole structure is high
- Since, the resonator vibrates in x and y directions, the electrodes are placed besides the structure instead of beneath it. So, the fabrication, mask defining, pattern generation and manufacturing of the device will be done more easily and inexpensively

**Frequency tuning:** Resonance frequency of the microresonator is a function of the dc-bias voltage  $V_p$ . Thus, frequency of this device is tunable via adjustment of  $V_p$  and this can be used advantageously to implement filters and oscillators with tunable center frequencies, or to correct for passband distortion caused by finite planar fabrication tolerances.

The dc-bias dependence of resonance frequency arises from a  $V_p$ -dependent electrical spring constant  $k_e$  that subtracts from the mechanical spring constant of the system  $k_m$ , lowering the overall spring stiffness  $k_r = k_m - k_e$ , thus lowering the resonance frequency according to the expression:

$$f_0 = \frac{1}{2\pi} \sqrt{\frac{k_m - k_e}{m_r}} = \frac{1}{2\pi} \sqrt{\frac{k_m}{m_r} \left[ 1 - \left( \frac{k_e}{k_m} \right) \right]} = \frac{\beta_n^2}{4\pi\sqrt{3}} \kappa \frac{W_r}{L_r^2} \sqrt{\frac{E}{\rho}} \left[ 1 - \left( \frac{k_e}{k_m} \right) \right]^{1/2} \quad (3)$$

where,  $k_m$  and  $m_r$  denote values at a particular location (usually the beam center location) and the quantity  $k_e/k_m$  must be obtained via integration over the electrode width  $W_e$  due to the location dependence of  $k_m$  as follows (Nathanson *et al.*, 1967):

$$\frac{k_e}{k_m} = \int_{L_{e1}}^{L_{e2}} \frac{V_p^2 \epsilon_0 h_r}{d^3(x) k_m(x)} dx \quad (4)$$

where, range of integration is from  $L_{e1} = 0.5(L_r - W_e)$  to  $L_{e2} = 0.5(L_r + W_e)$  and  $h_r$  and  $d(x)$  are structure thickness and gap between electrode and vibrating beam, respectively.

It must be noted that Eq. 3 is only valid for a case in which four outer electrodes are used. If in addition of four outer electrodes, four inner electrodes are also used (in order to reduce  $R_x$  further), then the term  $k_e/k_m$  in Eq. 3 should be multiplied by a factor of 2. In that case, the frequency  $f_0$  decreases further, with increasing  $V_p$ .

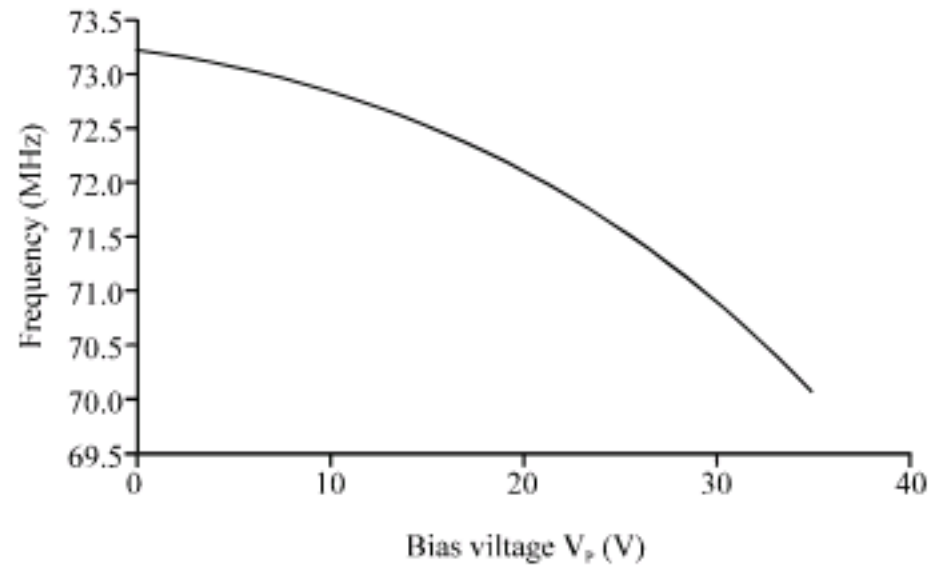


Fig. 4: Simulated frequency versus applied dc-bias  $V_p$  for the present microresonator

The dependence of the resonance frequency to dc-bias voltage  $V_p$ , is shown in Fig. 4.

**MOTIONAL RESISTANCE CALCULATION**

An electrical model with a core RLC circuit was defined for the microresonator based on mass-spring-damper system. Of the elements in the equivalent RLC circuit, the series motional resistance  $R_x$  is the most influential in both oscillator and filter circuits. In oscillators,  $R_x$  generally governs the gain needed to instigate and sustain oscillation; whereas in bandpass filters, it dictates the ease of matching the designed filter to low impedance stages before and after the filter (e.g., the antenna).

$$R_x = \frac{\sqrt{k_r m_r}}{Q \eta_c^2} = \frac{D_r}{\eta_c^2} \tag{5}$$

where,  $\eta_c$  is the transduction parameter for a capacitive transducer and is calculated theoretically as follows:

$$\eta_c = V_p \left( \frac{\partial C}{\partial x} \right) = \frac{V_p \epsilon_0 W_r W_c}{d_0^2} \tag{6}$$

and  $D_r$  is the damping factor which is given by:

$$D_r = \frac{\sqrt{k_m m_r}}{Q_{nom}} \tag{7}$$

where  $k_m$  and  $m_r$  denote the mechanical spring constant value and the equivalent mass of the system at the beam center location on the resonator and  $Q_{nom}$  is the quality factor of the resonator without the influence of applied voltages and electrodes.

To having better insight into what parameters governs  $R_x$ , a closed form expression can be obtained by

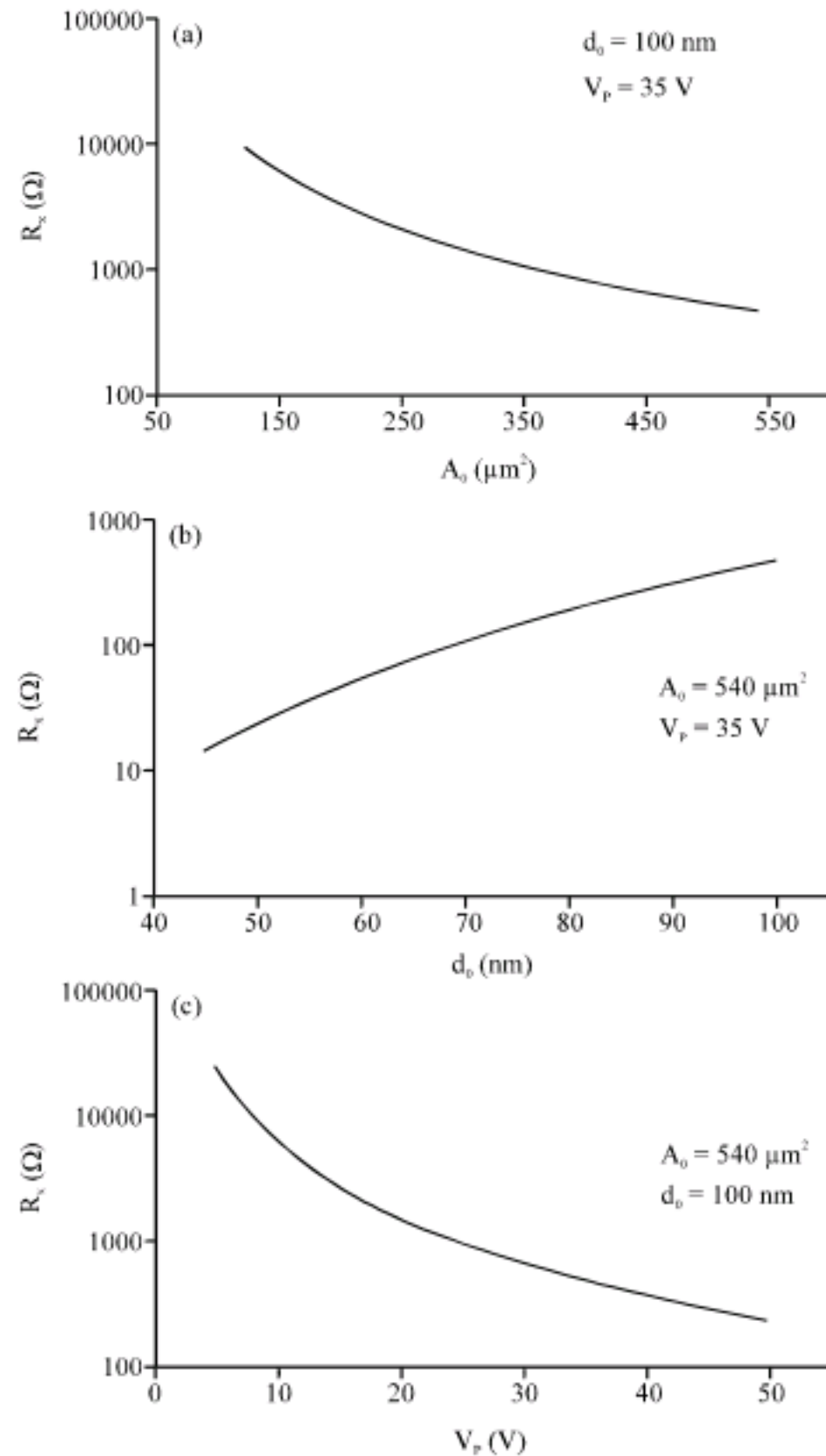


Fig. 5: Simulated plots presenting  $R_x$  values obtained via, Eq. 8. (a)  $R_x$  versus electrode-to-resonator overlap area  $A_0$ . (b)  $R_x$  versus electrode-to-resonator gap spacing  $d_0$ . (c)  $R_x$  versus dc-bias  $V_p$

substituting Eq. 6 into 5 and using lumped terms for integrated parameters, which yields:

$$R_x = \frac{D_r d_0^4}{\epsilon_0 A_0^2 V_p^2} \tag{8}$$

where,  $A_0$  is the effective electrode-to-resonator overlap area of the resonator.

Figure 5 present plots of  $R_x$  versus various parameters in Eq. 8, showing that small values of  $R_x$  are feasible if small values of electrode-to-resonator gap spacing  $d_0$  and large values of dc-bias  $V_p$  and sufficiently large electrode-to-resonator overlap area are used. However, the use of such values should not sacrifice linearity.

As indicated in Fig. 5a, by choosing  $d_0 = 100$  nm,  $V_p = 35$  V and using eight electrodes (four outer electrodes and four inner electrodes), motional impedance of  $R_x$  is reduced to  $478 \Omega$ ; which is a desirable value for a micromechanical resonator. Furthermore, as it was explained before, use of special design for the support beams prevents lowering quality factor of the flexural mode beam resonators. Hence, there will not be any decrease in  $Q$  and increase in  $R_x$  as a result.

It must be noted that in Fig. 5b and c, total electrode-to-resonator overlap area is equal to  $540 \mu\text{m}^2$  and overlap area for each electrode-resonator pair is only  $75 \mu\text{m}^2$ , which leads to a large pull-in voltage ( $\sim 180$  V).

### SUPPORT STRUCTURE DESIGN

The designed square frame mechanical resonator is supported by four flexural beams attached at its fundamental-mode node points (Fig. 2). Since, these beams are attached at node points, the support springs sustain no translational movement during resonator vibration (ideally) and thus, support (i.e., anchor) losses due to translational movements are greatly alleviated. Furthermore, with the recognition that the supporting flexural beams actually behave like acoustic transmission lines at the VHF frequencies of interest, flexural loss mechanisms can also be negated by strategically choosing support dimensions so that they present virtually no impedance to the simply supported beam. In particular, by choosing the dimensions of a flexural support beam such that they correspond to an effective quarter-wavelength of the resonator operating frequency, the solid anchor condition on one side of the support beam is transformed to a free-end condition on the other side, which connects to the resonator. In terms of impedance, the infinite acoustic impedance at the anchors is transformed to zero impedance at the resonator attachment points. As a result, the resonator effectively sees no supports at all and operates as if levitated above the substrate, devoid of anchors and their associated loss mechanisms.

Through appropriate acoustical network analysis, the dimensions of a flexural beam are found to correspond to a quarter-wavelength of the operating frequency when they satisfy the following expression:

$$L_s^2 = \frac{1}{4f_0} \frac{\beta_n^2}{4\pi\sqrt{3}} W_s \sqrt{\frac{E}{\rho}} \quad (9)$$

where,  $W_s$  and  $L_s$  are the width and length of the support beams, respectively,  $\beta_n = 4.730, 7.853, 10.996$  for the first

three modes of a clamped-clamped beam and  $f_0$  is the resonance frequency of the microresonator.

**Estimating quality factor:** The mechanical quality factor ( $Q$ ) of a resonator is:

$$Q = 2\pi \frac{W}{\Delta W} \quad (10)$$

where,  $\Delta W$  denotes the energy dissipated per cycle of vibration and  $W$  denotes the maximum vibration energy stored per cycle.

Many dissipation mechanisms exist in microelectromechanical resonators, such as air damping, thermoelastic damping (TED), surface loss and support loss. Unloaded  $Q$  of a microresonator is mainly the combination of these dissipation mechanisms, expressed as (Bannon III *et al.*, 2000):

$$\frac{1}{Q} = \frac{1}{Q_{\text{air}}} + \frac{1}{Q_{\text{TED}}} + \frac{1}{Q_{\text{Surface}}} + \frac{1}{Q_{\text{Support}}} \quad (11)$$

Thus, to determine  $Q$  of the designed resonator, it was necessary to calculate  $Q$  of each dissipation mechanisms as following:

$Q_{\text{air}}$  denotes the quality factor due to energy loss mechanisms of air damping and is determined as follows (Blom *et al.*, 1992; Cho *et al.*, 1993):

$$Q_{\text{air}} = \frac{k}{\omega_0 b} \quad (12)$$

where,  $k$  is stiffness of vibrating spring and  $b$  is damping coefficient of a rectangular parallel-plate geometries and has been derived from a linearized form of the compressible Reynolds gas-film equation as follows (Rebeiz, 2003; Cheng *et al.*, 2002):

$$b = \frac{3}{2\pi} \mu \frac{A^2}{d_0^3} \quad (13)$$

where  $\mu = 1.78 \times 10^{-5} \text{ kg m}^{-1} \text{ sec}^{-1}$  (for air in standard temperature and pressure (STP) conditions) is coefficient of viscosity and proportional to gas pressure and consequently mean free path of gas molecules (Abdelmoneum *et al.*, 2003).  $A$  and  $d_0$  are area of the device and gap between the two plates, respectively.

$Q_{\text{TED}}$  denotes the quality factor due to energy loss mechanisms of thermoelastic damping and is expressed as (Hao *et al.*, 2003; Braginsky *et al.*, 1985; Lifshitz and Roukes, 2000):

$$Q_{TED}^{-1} = \frac{E\alpha_T^2 T_0}{C_p} \frac{\omega\tau}{1 + (\omega\tau)^2}, \tau = \frac{C_p W_r^2}{C_T \pi^2} \quad (14)$$

where  $\alpha_T$  and  $C_p$  denote thermal expansion coefficient and specific heat at constant pressure of the material used for the beam, respectively;  $T_0$  is the environmental temperature and where  $C_T$  denotes thermal conductivity of the beam material and  $\omega$  denotes the angular frequency of the beam resonator.

$Q_{Surface}$  denotes the quality factor due to energy loss mechanisms of surface loss and the following expression it has been suggested for it (Hao *et al.*, 2003; Braginsky *et al.*, 1985):

$$Q_{Surface} = \frac{W_r h_r}{3W_r + h_r} \frac{E}{2E_{\delta s} \delta} \quad (15)$$

where,  $\delta$  denotes the characterized thickness of the surface layer and  $E_{\delta s}$  is a constant related to the surface stress (Yasumura *et al.*, 2000).

$Q_{Support}$  denotes the quality factor due to energy loss mechanisms of support loss and it can be calculated as follows (Mihailovich and MacDonald, 1995):

$$Q_{Support} = 2\pi \frac{KE_{tot}}{E_{loss}} \quad (16)$$

where,  $KE_{tot}$  is the stored flexural vibration energy for each resonant mode of a beam resonator can be expressed as (Cross and Lifshitz, 2001):

$$KE_{tot} = \frac{1}{2} m v^2 = \frac{1}{2} \rho h W_r L_r \omega_0^2 U_0^2 \quad (17)$$

where,  $\omega_0$  and  $U_0$  denote the fundamental angular frequency of the vibration and the vibration amplitude, respectively and  $E_{loss}$  is the energy dissipated per cycle of vibration through supports via., anchors to substrate and for a clamped-free beam is calculated as follows (Hao *et al.*, 2003; Hao and Ayazi, 2005):

$$E_{loss} = \frac{1.344}{Eh} \frac{1+\nu}{1-\nu} \Gamma_0^2 \quad (18)$$

where,  $\nu$  is Poisson ratio of the support material and  $\Gamma_0$  is a fundamental vibrating shear force on support where attached to substrate, which can be achievable by finite element analysis.

Plots of quality factor of the proposed microresonator versus electrode-to-resonator gap and versus ambient pressure are shown in Fig. 6 and 7, respectively.

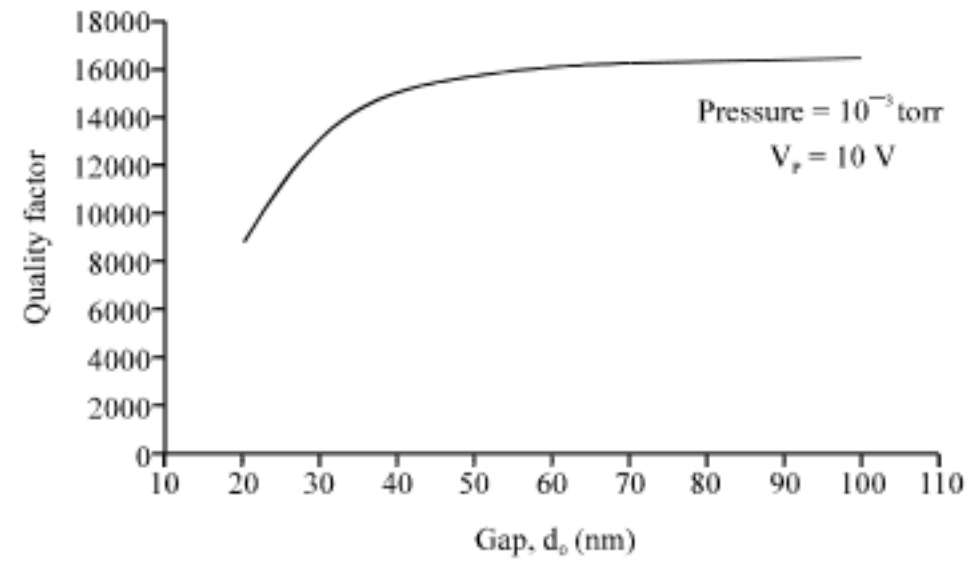


Fig. 6: Plot of Q versus electrode-to-resonator gap

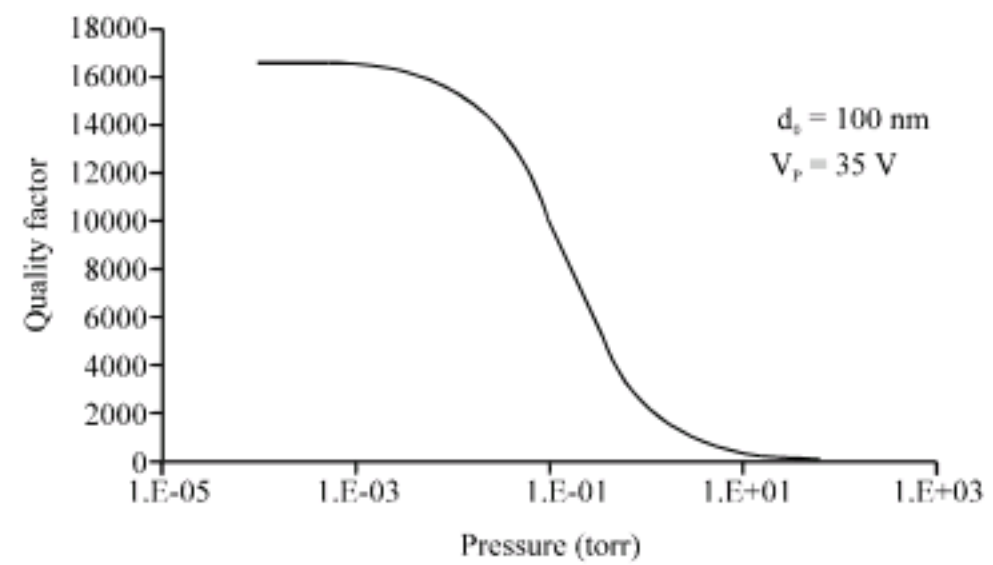


Fig. 7: Plot of Q versus ambient pressure of the microresonator

### MICROMECHANICAL RESONATOR CHARACTERISTICS

It must be noted that the simulated spectrum for the 71 MHz micromechanical resonator shown in Fig. 3 was related to the not properly terminated resonator and the transmission gain at the peak of the simulated frequency characteristic was determined from an impedance-mismatched single resonator circuit. So, the simulated transmission gain was not the same as insertion loss. Indeed, the transmission gain was calculated via., the following formula:

$$\text{Transmission Gain} = 20 \log \left( \frac{R_s + R_p}{R_L} \right) \quad (19)$$

where,  $R_p$  is the polysilicon interconnect series resistance.

The material properties used in this study and surrounding conditions of the resonator are shown in Table 1 (Hao *et al.*, 2003; Abdolvand *et al.*, 2006). Table 2 shown the simulated micromechanical resonator

Table 1: Material properties and surrounding conditions of the resonator

Parameters	Explanation	Value	Units
E	Young's modulus for polysilicon	150	GPa
$\rho$	Density of polysilicon	2,300	kg m <sup>-3</sup>
$\nu$	Poisson's ratio	0.28	-
$\alpha_T$	Thermal expansion coefficient	2.6×10 <sup>-6</sup>	K
C <sub>p</sub>	Specific heat	1.63×10 <sup>6</sup>	J K <sup>-1</sup> m <sup>-3</sup>
C <sub>T</sub>	Thermal conductivity	90	W m <sup>-1</sup> K <sup>-1</sup>
T <sub>0</sub>	Environmental temperature	300	K
$\mu$	Absolute viscosity of air	1.78×10 <sup>-5</sup>	kg m <sup>-1</sup> sec <sup>-1</sup>
P <sub>a</sub>	Ambient pressure	0.1	torr

Table 2: VHF micromechanical resonator summary

Parameters	Explanation	Value	Unit
f <sub>nom</sub>	Mechanical resonance frequency	71.7	MHz
f <sub>0</sub>	Center frequency	71	MHz
$\kappa$	Frequency modification factor	0.99274	-
L <sub>r</sub>	Average beam length	10	$\mu$ m
W <sub>r</sub>	Beam width	2	$\mu$ m
h <sub>r</sub>	Structural thickness	15	$\mu$ m
W <sub>c(out)</sub>	Outer electrode width	5	$\mu$ m
W <sub>c(in)</sub>	Inner electrode width	4	$\mu$ m
d <sub>0</sub>	Electrode to resonator gap	100	nm
L <sub>s</sub>	Support beam length	5.3	$\mu$ m
W <sub>s</sub>	Support beam width	1	$\mu$ m
h <sub>s</sub>	Support beam thickness	15	$\mu$ m
Q	Quality factor	9,912	-
m <sub>r</sub>	Resonator mass at middle of each beam	3.45×10 <sup>-13</sup>	kg
k <sub>m</sub>	Resonator stiffness at middle of each beam	72,000	N m <sup>-1</sup>
k <sub>e</sub>	Electrical spring constant	-676	N m <sup>-1</sup>
$\eta_e$	Transduction parameter	2.228×10 <sup>-6</sup>	C m <sup>-1</sup>
V <sub>p</sub>	DC-bias voltage	35	V
R <sub>s</sub>	Motional resistance	478	$\Omega$

Table 3: Calculated Q of each dissipation mechanisms and total Q of the resonator

Q <sub>Air</sub>	Q <sub>TED</sub>	Q <sub>Surface</sub>	Q <sub>Support</sub>	Q <sub>Total</sub>
24,955	19,500	126,050	625,572	9,912

characteristics and finally, the calculated quality factor of the resonator and each of dissipation mechanisms are presented in Table 3.

### CONCLUSION

Design and simulation of a VHF micromechanical resonator based on the new structure square frame suitable for operating around 71 MHz is reported. The proposed microresonator exhibits series motional resistances considerably smaller than that of other beam resonators by a factor equal to the number of electrodes used in each resonator. The present method for R<sub>s</sub>-reduction does not degrade linearity of the resonator and in contrast to arrayed microresonators does not consume chip area anymore. This technique alleviates some of remaining challenges that slow the advancement in integration resonators, filters and oscillators into communication systems and helps realization of a single-chip, fully integrated communication system based on RF MEMS technology.

### ACKNOWLEDGMENT

This research was supported by Iran Telecommunication Research Center (ITRC).

### REFERENCES

- Abdelmoneum, M.A., M.U. Demirci and C.T.C. Nguyen, 2003. Stemless wine-glass mode disk micromechanical resonators. Proceeding of IEEE the 6th Annual International Conference on Micro Electro Mechanical Systems, Jan. 19-23, IEEE Press, Kyoto, Japan, pp: 698-701.
- Abdolvand, R., H. Johari, G.K. Ho, A. Erbil and F. Ayazi, 2006. Quality factor in trench-refilled polysilicon beam resonators. *J. Microelectromech. Syst.*, 15: 471-478.
- Alastalo, A.T. and V. Kaajakari, 2006. Third-order intermodulation in microelectromechanical filters coupled with capacitive transducers. *J. Microelectromech. Syst.*, 15: 141-148.
- Bannon III, F.D., J.R. Clark and C.T.C. Nguyen, 2000. High-Q HF microelectromechanical filters. *IEEE J. Solid St Circ.*, 35: 512-526.
- Blom, F.R., S. Bouwstra, M. Elwenspoek and J.H.J. Fluitman, 1992. Dependence of the quality factor of micromachined silicon beam resonators on pressure and geometry. *J. Vac. Sci. Technol. B*, 10: 19-26.
- Braginsky, V.P., V.P. Mitrofanov and V.I. Panov, 1985. Systems with Small Dissipation. 1st Edn., The University of Chicago Press, London, ISBN: 0226070735.
- Cheng, Y.T., W.T. Hsu, L. Lin, C.T.C. Nguyen and K. Najafi, 2002. Vacuum packaging technology using localized aluminum/silicon-to-glass bonding. *J. Microelectromech. Syst.*, 11: 556-565.
- Cho, Y.H., B.M. Kwak, A.P. Pisano and R.T. Howe, 1993. Viscous energy dissipation in laterally oscillating planar microstructures: A theoretical and experimental study. Proceedings of the 6th International Conference on Micro Electro Mechanical Systems, Feb. 7-10, IEEE Press, pp: 93-98.
- Cross, M.C. and R. Lifshitz, 2001. Elastic wave transmission at an abrupt junction in a thin plate with application to heat transport and vibrations in mesoscopic systems. *Phys. Rev. B*, 64: 1-22.
- De Los Santos, H.J., 2002. RF MEMS Circuit Design for Wireless Communications. 1st Edn., Artech House, Boston, ISBN: 1-58053-329-9.



- Demirci, M.U., M.A. Abdelmoneum and C.T.C. Nguyen, 2003. Mechanically corner-coupled square microresonator array for reduced series motional resistance. Proceedings of the 12th International Conference on Solid State Sensors, Actuators and Microsystems, June 8-12, IEEE Press, Massachusetts, Boston, pp: 955-958.
- Hao, Z., A. Erbil and F. Ayazi, 2003. An analytical model for support loss in micromachined beam resonators with in-plane flexural vibrations. *Sensor. Actuat. A Phys.*, 109: 156-164.
- Hao, Z. and F. Ayazi, 2005. Support loss in micromechanical disk resonators. Proceeding of the 18th IEEE International Conference on Micro Electro Mechanical Systems, 30 Jan. -3 February, IEEE Press, Miami Beach, Florida, pp: 137-141.
- Lifshitz, R. and M.L. Roukes, 2000. Thermoelastic damping in micro- and nanomechanical systems. *Phys. Rev. B*, 61: 5600-5608.
- Mihailovich, R.E. and N.C. MacDonald, 1995. Dissipation measurements of vacuum operated single-crystal silicon microresonators. *Sensor. Actuat. A Phys.*, 50: 199-207.
- Nathanson, H.C., W.E. Newell, R.A. Wickstrom and J.R., Jr. Davis, 1967. The resonant gate transistor. *IEEE Trans. Electron Dev.*, ED-14: 117-133.
- Navid, R., J.R. Clark, M. Demirci and C.T.C. Nguyen, 2001. Third-order intermodulation distortion capacitively-driven CC-beam micromechanical resonators. Proceedings of the 14th IEEE International Conference on Micro Electro Mechanical Systems, Jan. 21-25, IEEE Press, Interlaken, Switzerland, pp: 228-231.
- Nguyen, C.T.C., 1998. Microelectromechanical devices for wireless communications. Proceedings of the 11th Annual International Workshop on Micro Electro Mechanical Systems, Jan. 25-29, IEEE Press, Heidelberg, Germany, pp: 1-7.
- Nguyen, C.T.C., 1999. Frequency-selective MEMS for miniaturized low-power communication devices. *IEEE Trans. Theory Techniques*, 47: 1486-1503.
- Rebeiz, G.M., 2003. *RF MEMS: Theory, Design and Technology*. 1st Edn., John Wiley and Sons. New Jersey, ISBN: 0-471-20169-3.
- Timoshenko, S., D.H. Young and W. Weaver, 1974. *Vibration Problems in Engineering*. 4th Edn., John Wiley and Sons, New York, ISBN: 0471873152.
- Varadan, V.K. and K.J. Vinoy, 2002. *RF MEMS and their Applications*. 1st Edn., John Wiley and Sons, New York, ISBN: 0-470-84308-X.
- Wang, K., A.C. Wong and C.T.C. Nguyen, 2000. VHF free-free beam high-Q micromechanical resonators. *J. Microelectromech. Syst.*, 9: 347-360.
- Yasumura, K.Y., T.D. Stowe, E.M. Chow, T. Pfafman and T.W. Kenny *et al.*, 2000. Quality factors in micron- and submicron-thick cantilevers. *J. Microelectromech. Syst.*, 9: 117-125.